Validating an Isolator to Eliminate Grounding Issues for High-Resolution Digitizer Measurements

Peter N. Davis and Paul S. Wright

***Abstract*— This article describes a method of isolating high-resolution digitizers that have a common ground between channels. Isolation enables the digitizers to be used simultaneously to measure multiple points in a circuit without short-circuiting via the common ground. The isolators, when used in a switch formation, provide a method to cancel out the phase angle errors when measuring the difference in phase angles between channels. Various tests are reported, which assess the performance of the isolator over its operating range. These include temperature coefficient, linearity, gain stability common-mode rejection, and crosstalk.**

***Index Terms*— Electromagnetic compatibility, isolators, power measurement, power quality, wattmeters.**

I. Introduction

HIGH-RESOLUTION digitizers have the frequency bandwidth and high precision to undertake a wide range of electrical measurements; however, these digitizers have a common safety earth connection on the outer low terminals of their BNC connector inputs. This grounding point makes it difficult to simultaneously measure two outputs of an electrical circuit, such as those that would be typically required in a power or impedance measurement. This is because the common low inputs create a short-circuit across the network that they are measuring. Isolation is possible using an isolation transformer [1], but these can reduce the bandwidth of voltage measurement. Previous work at the U.K. National Physical Laboratory (NPL) has created isolation transformers for wattmeters up to 30 kHz [2]. However, a wider bandwidth isolation transformer is necessary to make full use of the digitizer frequency range.

Using digital sampling techniques for high-precision power is a common technique among national metrology institutes (NMIs) [3]. Isolation between channels can be designed to include power supplies isolating each channel. Some off-the-shelf digitizers do not have isolation, but the digitizers have a proven bandwidth and resolution to undertake precise wideband power measurements [4].

Isolation can be provided by the transducers used with the digitizer, voltage transformers can be used to step down the voltage and provide galvanic isolation. Current transformers and other current transducers also provide isolation between the measurement device and circuit under test. However, any future NPL wideband wattmeter would use the very low-frequency response provided by both resistive voltage dividers [5], and current shunts provide [6]. These transducers lack isolation, and therefore, an external analog isolator is necessary.

Analog isolation is possible through different physical processes; the previous work at NPL was undertaken using linear optical isolators [2]. Manufacturers, such as Texas Instruments, use capacitive coupling in their IS0124 analog isolator [7] and techniques to isolate the signals using magnetic coupling [8] also exist. This article utilizes the AD215 Isolator that has sufficient bandwidth for the measurements required, within the AD215 isolator a transformer provides isolation with the signal being modulated and demodulated across the transformer [9].

This article is an extension of the proceedings paper [10] and expands on the switching isolator design and principles of operation, before identifying further measurements that are necessary to characterize the switching isolator. For each set of measurements, the experimental setup is described, results are given, and conclusions are drawn. Finally, the uncertainties of each test are compared, and future developments are suggested.

II. Switching Isolator

If measurements were electrically isolated from the circuit under test, then the problem of a common grounding point on the digitizer would be eliminated. Linear isolators provide good common-mode rejection and isolation but unfortunately introduce a phase delay. This phase delay will have an impact on measurements that require a phase angle, such as power and impedance. In circumstances where phase angle is important, for example, in a power measurement circuit, the isolators can be interchanged. One such setup is shown in Fig. 1 where a pair of AD215 linear isolation amplifiers were used with relays on either side of the AD215s. The latched contact relays (Axicom V23079 [11]) were chosen based on their high

Manuscript received October 11, 2020; revised December 3, 2020; accepted December 18, 2020. Date of publication January 8, 2021; date of current version February 2, 2021. This work was supported in part by the EMPIR Programme within the EMPIR project 17NRM02 MeterEMI co-financed by Participating States and in part by the European Union's Horizon 2020 Research and Innovation Programme. The Associate Editor coordinating the review process was Dimitrios Georgakopoulos. *(Corresponding author: Peter N. Davis.)*

The authors are with the National Physical Laboratory, Teddington TW11 0LW, U.K. (e-mail: peter.davis@npl.co.uk).

Digital Object Identifier 10.1109/TIM.2020.3048517

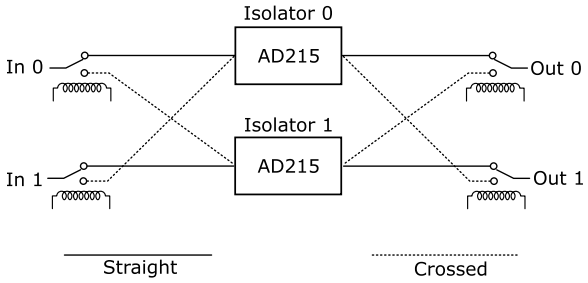

Fig. 1. Schematic layout of isolators and relays indicating straight and crossed signal paths.

isolation at the frequency and low insertion loss. Alternative isolators and relays may be implemented in this switched formation but may present different results. A microcontroller was implemented to control the relays providing two paths for the signal, a straight path (named "straight"), where In 0 is connected to Out 0 via Isolator 0 and, similarly, In 1 is connected to Out 1 through Isolator 1. The second path, named "crossed," connects the signal In 0 to Out 0 via Isolator 1 and connects In 1 to Out 1 via Isolator 0.

Interchanging the isolators enables calculating a difference in input phase angle, both in the straight and crossed paths. The average of the straight and crossed phase measurements eliminates the phase error from the power measurement to a first-order approximation, as shown in the following equation:

$$\phi_{\text{in0}} - \phi_{\text{in1}} = \frac{(\phi_{\text{out0s}} - \phi_{\text{out1s}}) + (\phi_{\text{out0c}} - \phi_{\text{out1c}})}{2} \quad (1)$$

where ϕ_{in0} and ϕ_{in1} are the phase angles of In 0 and In 1, respectively, ϕ_{out0s} and ϕ_{out1s} are the phase angles of Out 0 and Out 1, respectively, when the isolators are in the straight configuration, and ϕ_{out0c} and ϕ_{out1c} are the phase angles of Out 0 and Out 1, respectively, when the isolators are in the crossed configuration. The switching technique has been previously applied to eliminate phase angle drift in the wattmeter [2].

III. Identification of Further Measurements

The introduction of the switching isolator will cause further measurement complexities. This section identifies the problems that need to be quantified for the isolator to be useful in electrical measurements.

A. Phase Angle

The canceling of phase angle errors in the isolator should be achieved through the switching of the isolators, as shown in Section II. To determine if there are any residual phase angle errors and to show that the switching isolator is working correctly, measurements need to be undertaken to test the limits of the correction.

B. Impact of Temperature on Gain

The AD215 has a change of gain with the temperature of 0.018% between 20 °C and 30 °C, based on the datasheet [9]. The circuit surrounding the isolator to modify the gain and adjust output offset will also be susceptible to temperature. The gain of the whole isolator circuit will be measured while changing the temperature of the isolator to determine whether any mitigating temperature control is necessary.

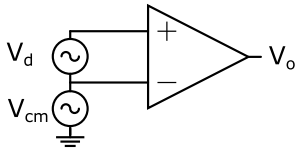

Fig. 2. Common-mode voltage and differential voltage.

C. Common-Mode Effects

Any practical differential amplifier, as shown in Fig. 2, depends not only on the differential signal (V_d) but also any common signal present on both inputs (V_{cm}). Measuring the common-mode rejection ratio (CMRR) of the isolator is an important stage in quantifying how much of the output signal is the desired differential signal and how much is from the undesired common mode.

D. Crosstalk Effects

One application for the isolator would be implementing a wattmeter with voltage and current components up to 100 kHz. If using real-world nonsinusoidal current waveforms with short rise times, then there could be crosstalk between channels, and the sharp edges of the current waveform may present on the voltage waveform (or vice versa). Testing needs to be undertaken to measure if there is any crosstalk between the channels and to quantify it.

E. Linearity

The AD215 isolator datasheet describes [9] a nonlinearity of 1 mV across the whole −10–+10 V_p range. The digitizer that the isolator will be used with has a voltage range of 10 V_{pp}, so any nonlinearity over this range needs to be identified with potential corrections.

F. Impact of Frequency on Gain

The AD215 isolator implements a 150-kHz low-pass filter on its output, which changes the gain as frequency increases. It is important to also measure the stability of the frequency response to understand if correction is feasible.

IV. Undertaking Further Measurements

For each of the problems highlighted in Section III, measurements have been undertaken to quantify the uncertainty. This will be expressed through an explanation of the experimental setup, results, and conclusions drawn.

A. Phase Angle

1) Experimental Setup: In order to determine the isolator amplitude stability and check the elimination of the phase error, the switching isolator was placed in a test circuit, as shown in Fig. 3. A Fluke 5700 voltage calibrator is used to

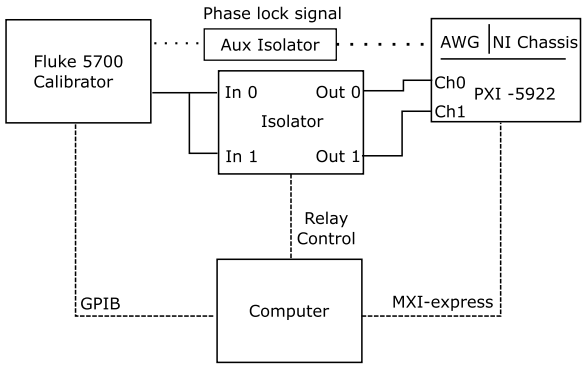

Fig. 3. Test circuit to measure the amplitude and phase–frequency response of the isolator. Full lines represent voltage signals, and dashed lines represent control signals.

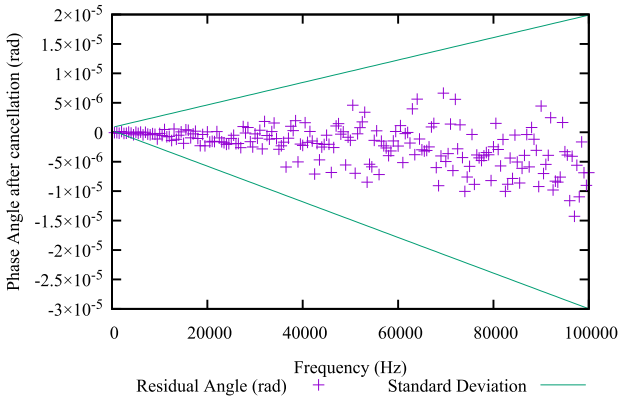

Fig. 4. Residual phase angle between isolators after switching and canceling, including linear fits of results + standard deviation and results—standard deviation.

supply the same voltage into both Input 0 and Input 1 of the isolator. Output 0 and Output 1 of the isolator were connected to Channel 0 and Channel 1 of the digitizer, in this case, an NI PXI-5922, to undertake an in-phase measurement. To ensure phase locking between the calibrator and the sampling frequency of the PXI-5922, an arbitrary waveform generator (in the same NI Chassis as the PXI-5922) was used to generate a phase-locking signal. A computer was used to control the NI chassis (via the MXI-express), the isolator relays, and the voltage calibrator using the GPIB. The voltage calibrator has been calibrated using ac/dc at various frequencies from 50 Hz to 100 kHz at 0.7 V. Using the corrections from the calibration, an interpolation was applied between these calibrated frequencies. The calibrator output was varied from 500 Hz to 100 kHz in steps of 500 Hz, and the outputs of the isolator were sampled at 1 MSa/s using the digitizer.

2) Results: For each frequency run, a fast Fourier transform (FFT) was calculated, and the amplitude and phase of the applied frequency were recorded. The frequency run was repeated multiple times, the results were averaged, and the standard deviation was obtained. Fig. 4 shows the residual phase angles after applying the cancellation described in Section II, giving an absolute maximum phase error of less than 15 μrad. The standard deviation for the measurements is

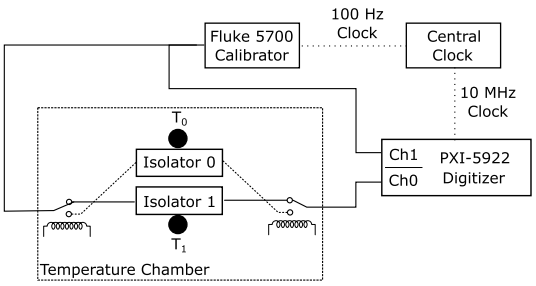

Fig. 5. Test circuit to measure the impact of temperature on the gain of the isolator. Full lines represent voltage signals, and dotted lines represent clock signals.

represented in Fig. 4 by fitting linear lines to the standard deviation data, which gives a range of −30–+20 μrad for the 100 kHz. In comparison to this, the drift of phase angle between two AD215s when not in a switched configuration was 5 μrad over a 30 min for a 100-Hz signal.

B. Impact of Temperature on Gain

1) Experimental Setup: The switching isolator was placed inside a temperature chamber with a measurement circuit, as shown in Fig. 5. The temperature chamber was set to a range of temperatures from 18 °C to 33 °C with 2.5 °C intervals. At each set point, the chamber was left to stabilize. As shown in Fig. 5, a Fluke 5700 calibrator was used to apply 3 V at 100 Hz to the input of the isolator, and the output of the isolator was measured by channel 0 of the PXI-5922 digitizer; 100 Hz was applied to reduce any background frequency from the mains. The input of the isolator was also measured directly on the PXI-5922 digitizer. To provide phase locking between the calibrator and digitizer, a central clock generated signals for both, as shown in Fig. 5. In order to measure the temperature of each isolator, a temperature measurement sensor (DS18B20) was placed in contact with the surface of the isolator. The isolator was switched between the crossed and straight configuration shown in Fig. 1 to measure both isolators. A PC was used to control the isolator, record measurements from the PXI-5922 digitizer, and log the values from the temperature sensors.

2) Results: An FFT was applied to the digitizer data, and the fundamental of the FFT was obtained for both the input and output of the isolator. The gain was calculated using the ratio. Measurements for each temperature sensor were averaged, and a standard deviation was applied to check for stability in temperature readings. Fig. 6 shows the gain against temperature for both isolators.

Both isolators show a change in gain with temperature, with the greatest gradient being less than 14 ppm/°C. To mitigate this coefficient, temperature control of the isolator can be used to minimize the uncertainty in the gain. If the temperature can be controlled to stability of ±0.5 °C, the uncertainty on gain due to temperature could then be conservatively assessed at 14 ppm. The difference in isolators' temperature/gain gradient shows that there is a benefit in searching for isolators that have a matched gradient.

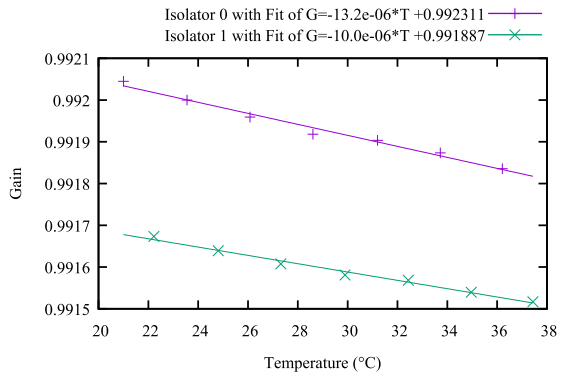

Fig. 6. Measured gain of isolator 0 and isolator 1 for various temperatures. Trend lines for both isolators are shown with gradients of −13.2 and −10.0 ppm/°C for isolator 0 and isolator 1, respectively.

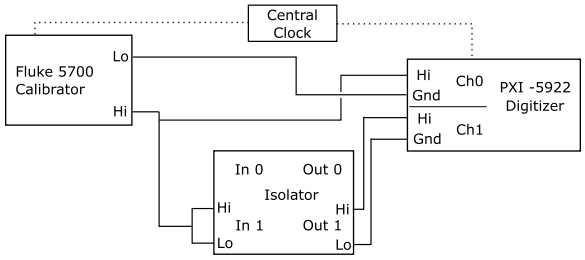

Fig. 7. Equipment setup for common-mode testing. Full lines represent voltage signals, and dotted lines show clock signals.

C. Common-Mode Effects

1) Experimental Setup: The experimental setup to measure the effect of the common mode is shown in Fig. 7. To create a common-mode signal, both the high and low of the In1 of the isolator were applied with the high output of voltage generated by a Fluke 5700 calibrator. The Fluke 5700 calibrator output was set to 3 V, and the frequency was varied from 1 to 100 kHz in 1-kHz increments. The calibrator voltage was applied to channel 0 of the PXI-5922 digitizer (10-V_{pp} range), and the output was also applied to both high and low inputs of one of the channels (In1). Out1 of the isolator fed into channel 1 of the PXI-5922 (2-V_{pp} range). For frequency locking, a central clock provided timing signals for both the calibrator and the digitizer. The digitizer sampled at 1 Msa/s. The isolator was switched between straight and crossed formation (shown in Fig. 1) to test both isolator 0 and isolator 1.

2) Results: The CMRR is shown in Fig. 8 for the two isolators. Isolator 1 is consistently better by 1.9 dB over the whole range of the testing.

To determine the CMRR, the common-mode gain needs to be compared with the differential gain. The differential gain is determined in Section IV-F, and the impact of frequency on gain [12] is

$$\mathrm{CMRR(dB)} = 20\log_{10}\left(\frac{A_d}{A_{\mathrm{cm}}}\right) \tag{2}$$

where the differential gain A_d [12] is determined by dividing voltage out over voltage in for a system with as little common signal as possible

$$A_d = \frac{V_o}{V_{\mathrm{in}}}. \tag{3}$$

The common-mode A_{cm} [12] is determined by the dividing twice the voltage out by the common-mode voltage in, for a system with as little differential signal as possible

$$A_{\mathrm{cm}} = \frac{2V_o}{V_{\mathrm{in}}}. \tag{4}$$

An FFT was applied to the digitizer data, and the amplitude of the applied frequency was measured with channel 0. The amplitude of the applied frequency through the isolator was determined, and the average and standard deviation of multiple results were found and are shown in Fig. 9. As the standard deviation is too small to see clearly in Fig. 9, Fig. 10 shows the standard deviation across the frequency range.

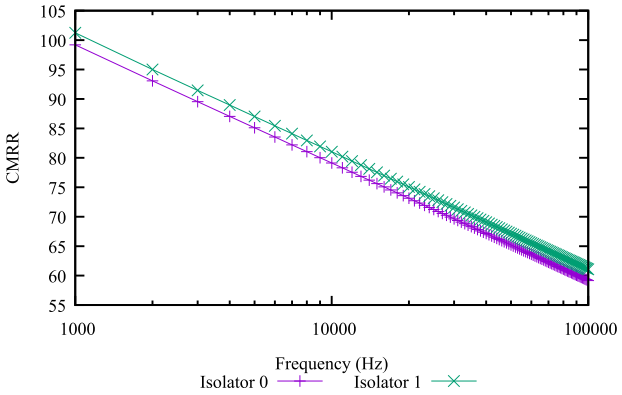

Fig. 8. CMRR of the two isolators in the frequency range of 1–100 kHz.

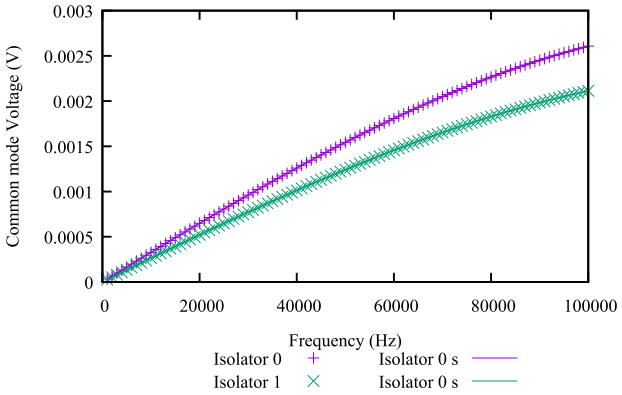

Fig. 9. Measured output voltage of both isolators and standard deviations bands when energized with a 3-V common-mode voltage. As the standard deviation envelope is difficult to distinguish from data, it is shown separately in Fig. 10.

D. Crosstalk Effects

1) Experimental Setup: The experimental setup to measure the effect of crosstalk is shown in Fig. 11. If the isolator has no input, this would make an op-amp on the input open-circuit, which would generate spurious results. A battery was applied

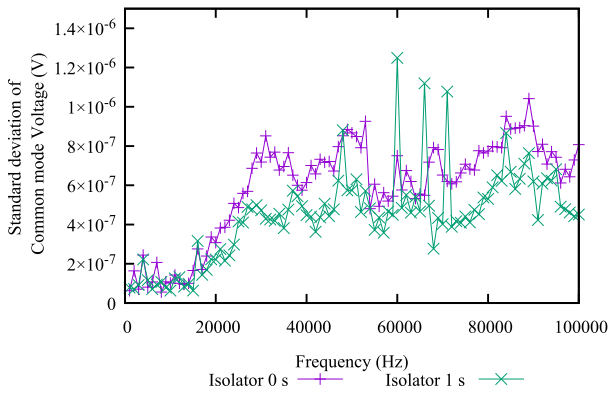

Fig. 10. Standard deviations of both the common-mode rejection measurements from both isolators.

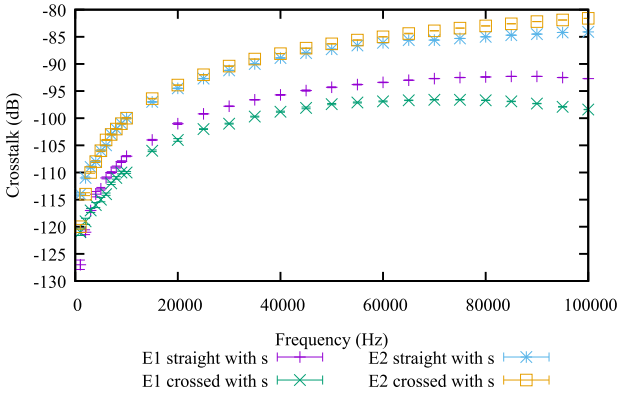

Fig. 12. Measurement crosstalk dB voltage from sinusoidal test signals applied at E1 and E2 in the crossed and straight positions.

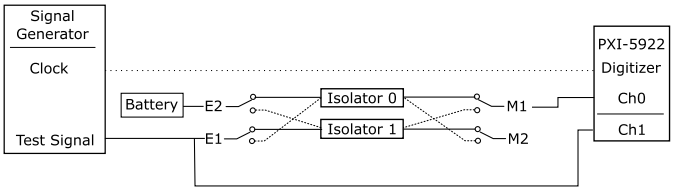

Fig. 11. Setup for crosstalk measurements when applying the test signals to E1 in straight or crossed mode; crosstalk is measured at M1. Similarly, when applying the test signal to E2 in both straight or crossed mode, crosstalk is measured at M2. Solid lines: voltage signals. Dotted lines: clock signals.

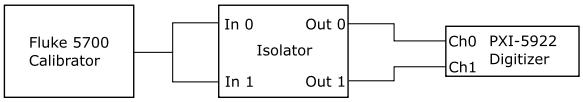

Fig. 13. Equipment setup to measure dc linearity of the isolator.

to the isolator under test to both eliminate the open-circuit and elicit a dc response from the isolator but not generate any frequency components, which could be measured as crosstalk. Crosstalk was measured using test signals consisting of sinewaves of frequencies 1–10 kHz in 1-kHz steps and 10–100 kHz in 5-kHz steps. In the straight configuration, the isolator was energized with the test signal from point E1 and the battery from E2 and measured from point M1. The point of energization was changed to E2 for the test signal and E1 for the battery, and the measure point was M2. For both configurations, the device was also tested in the switched configuration.

2) Results: An FFT was applied to the digitizer data, and the amplitude of the measured signal was calculated at the frequency of the input test signal. A ratio of the measured signal to test signal amplitude was calculated. Fig. 12 shows the measured crosstalk ratio with standard deviations. The results show that energizing E2 with the isolator in either a crossed or straight position creates crosstalk of -84 and -82 dB at 100 kHz, whereas energizing E1 the crosstalk is lower -93 and -98 dB for straight and crossed, respectively. The maximum standard deviation from either isolator is 0.4 μV/V.

The measured crosstalk will add to the uncertainty of both isolator measurements, but how the application of the switching isolator in a test circuit is controllable. In wideband electrical power measurements, the voltage is normally at the power frequencies of 50 or 60 Hz, and the current has higher frequency components. Implementing the switched isolator with the voltage entering E2 where most of the signal is 50/60 Hz, and current measurements using E1 would reduce the impact of crosstalk on the overall uncertainty. Crosstalk may be significantly improved by modifying the board layout, while normal trace routing procedures that followed further guard traces could be implemented to reduce the measure crosstalk.

E. Linearity

The isolator will be primarily used for ac measurements. However, the isolator does provide dc coupling, and the explanation of any ac nonlinearity may be assisted with an understanding of the dc nonlinearity.

1) DC Experimental Setup: The experimental setup to measure the isolator dc linearity is shown in Fig. 13. A Fluke 5700 voltage calibrator provides voltages from +4.5 to −4.5 V in 0.3-V steps to the inputs of both isolators simultaneously. The output of the isolators was measured by channels 0 and 1 of the digitizer, respectively. This measurement will also measure any nonlinearity of the digitizer. To remove the nonlinearity of the digitizer, the measurement is repeated without the isolator, and this nonlinearity is removed from the isolator characterization.

2) DC Results: The digitizer results were averaged for each amplitude and run; then, an average of multiple runs and a standard deviation was calculated. Fig. 14 shows the results of measured voltage against applied voltage, with the residual voltage once the linear component is removed. These data exceed the AD215 datasheet [9] where these measurements give a nonlinearity exceeding 1 mV, but the datasheet does not exceed 0.8 mV.

3) AC Experimental Setup: The experimental setup to measure the ac isolator linearity is shown in Fig. 15. A 3-V 1-kHz signal was generated from a Fluke 5700 calibrator. An IVD was used to step down the voltage from the calibrator giving

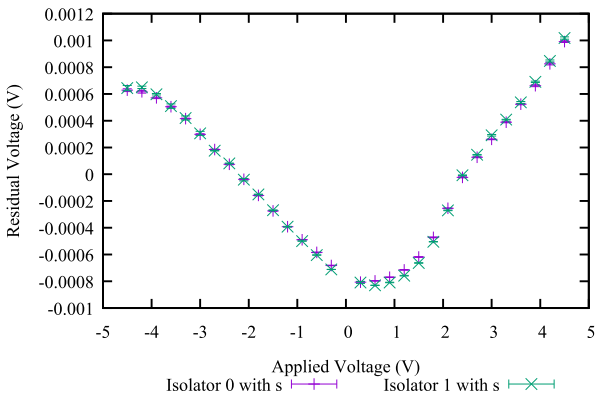

Fig. 14. Residual dc voltages after removing linear component for both isolator 0 and isolator 1 with error bars displaying standard deviation.

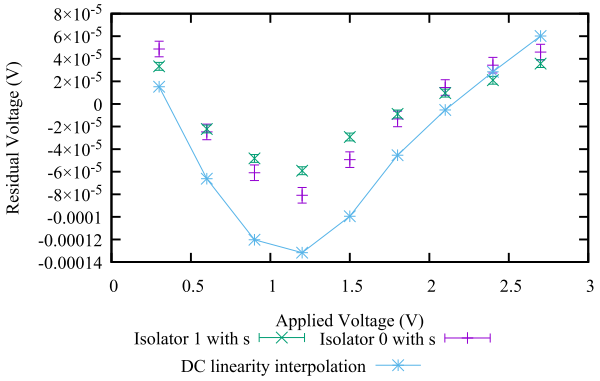

Fig. 16. Residual ac voltage of the isolator 0 and isolator 1 with error bars calculated from the standard deviation. The theoretical values calculated from dc linearity interpolation.

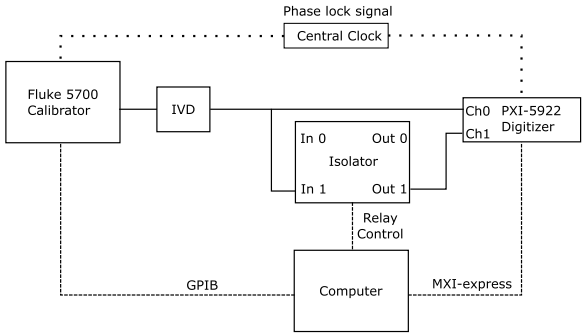

Fig. 15. Equipment setup to measure the ac linearity of isolator. Solid lines: voltages. Dashed lines: communications. Dotted lines: clock.

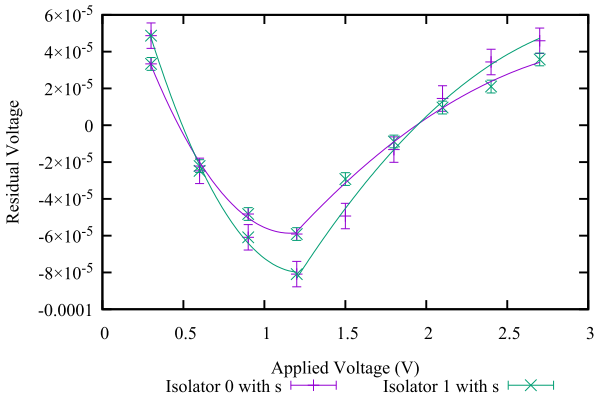

Fig. 17. Corrections for nonlinearities in the data and standard deviations. The fitted polynomials are: Isolator 0: $f(0.3 < V < 1.2) = 1.250 \times 10^{-4}$ V^2 $- 2.889 \times 10^{-4}$ V$+1.082 \times 10^{-4}$ and $f(1.2 < V < 2.7) = 3.27 \times 10^{-5}$ V$^2+ 2.147 \times 10^{-4}$ V $- 2.936 \times 10^{-4}$. Isolator 1: $f(0.3 < V < 1.2) = 1.356 \times 10^{-4}$ V$^2-3.427 \times 10^{-4}$ V$+1.356 \times 10^{-4}$ and $f(1.2 < V < 2.7) = -2.2 \times 10^{-5}$ V$^2 + 1.479 \times 10^{-4}$ V $- 2.033 \times 10^{-4}$.

the various amplitudes. The IVD was characterized with less than 1 μV/V on the range used providing higher linearity than the voltage calibrator. The output of the IVD was both applied to channel 0 of the digitizer (PXI5922) and to In1 of the isolator. Out1 of the isolator was measured with channel 1 of the digitizer. The setup was operated in both straight and crossed modes to test both isolators. A central clock provided timing signals for both the calibrator and digitizer.

4) AC Results: An FFT was applied to the digitized data, and the relevant bin for the 1-kHz signal was used. The amplitude of the voltage signal was calculated, and a linear regression was fitted for the known ratios on the IVD. The residual was calculated by subtracting the theoretical from the measured value. The results of multiple runs were averaged and a standard deviation was found; the results are shown in Fig. 16, with the maximum standard deviation for each isolator shown.

To aid in finding a suitable equation to fit the ac nonlinearity, the ac nonlinearity is also compared with the dc linearity test from Section IV-E2. The dc nonlinearity data were interpolated between each point using a spline. The dc nonlinearity was then calculated for equally spaced discrete points on a pure sinewave. The amplitude of the pure sinewave was varied to match the amplitudes that ac linearity was measured at. The root mean square of the sum of the sinewave and theoretical dc nonlinearity was calculated. The nonlinearity of the root mean squares was calculated and shown in Fig. 16.

The interpolated dc linearity shows a similar shape to measured ac nonlinearity. This indicates that the cause of ac nonlinearity is mostly from the dc nonlinearity. Further corrections from the curve fitting in Fig. 17 were applied to the previously measured residual voltage. The maximum absolute deviation with the further correction applied gave a residual voltage of 4 μV.

F. Impact of Frequency on Gain

1) Experimental Setup: The experimental setup to measure the impact of frequency on the gain of the isolator is shown in Fig. 18. The calibrator is used to energize the inputs of the isolator with sinewave voltages in the frequency range from 1 to 100 kHz, in steps of 1 kHz. The calibrator was calibrated using ac/dc at 3 V for various spot frequencies, with an uncertainty of 25 μV/V in the range 50–100 kHz. The values for every 1 kHz were interpolated. The calibrator was

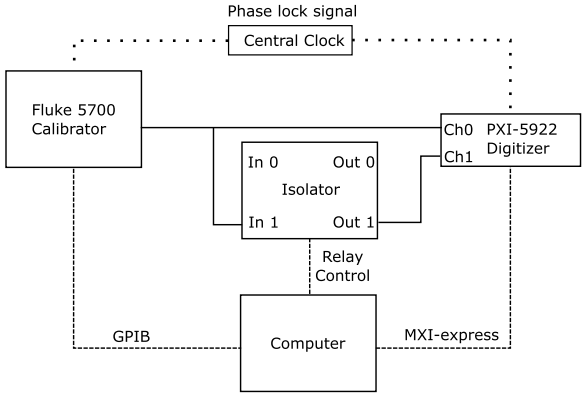

Fig. 18. Test circuit to measure the impact of the gain on frequency. Full lines: voltage signals. Dotted lines: clock signals.

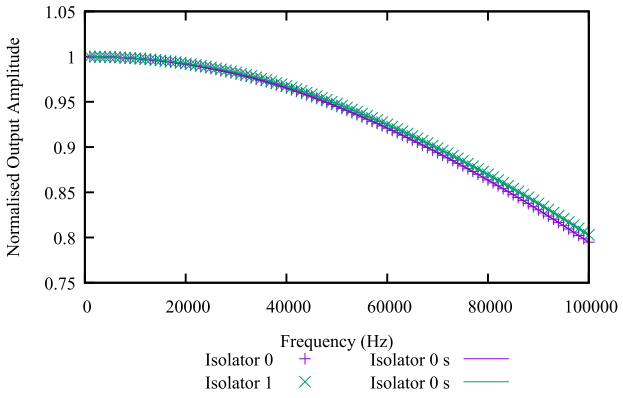

Fig. 19. Normalized output amplitude against frequency and standard deviation of results as standard deviation envelope is difficult to see and these are replotted on their own in Fig. 20.

connected to channel 0 of the digitizer card (PXI-5922) and into input 1 of the isolator or into channel 1 of the digitizer. For each frequency, a measurement was taken with both the straight configuration and the crossed configurations to obtain results for both AD215 isolators.

2) Results: An FFT was applied to the digitizer data. The amplitude of the frequency under test was determined, and both the mean and standard deviation were calculated for multiple runs. The results were then normalized to the 1-kHz measurement. Fig. 19 shows the normalized output and the standard deviation of the repeats, and due to the small magnitude of the standard deviation envelope, these are expanded in Fig. 20.

The two normalized values of the isolators are 1% different in value at 100 kHz. The gains of the isolators at 10 kHz are 0.997990 and 0.998158 for isolator 0 and isolator 1, respectively, with standard deviations less than 4 μV/V. By 30 kHz, the gains are 0.980992 and 0.982420 for isolators 0 and 1, respectively, with standard deviations of less than 12 μV/V. At 100 kHz, the gains become 0.794841 and 0.802824 for isolators 0 and 1, respectively, with isolator 0 having a standard deviation of 85 μV/V and isolator 1 having a standard deviation of 55 μV/V. The datasheet for the AD215 [9] gives a −2-dB gain at 100 kHz and the measured gain on the isolators

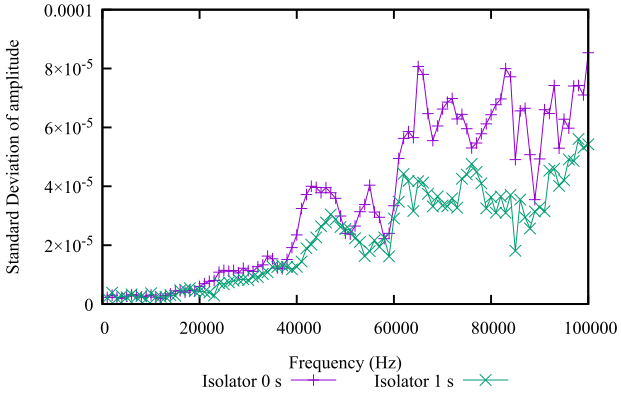

Fig. 20. Standard deviation of amplitudes for isolator 0 and isolator 1 across frequency sweep.

at 100 kHz are −2.07 and −1.96 dB for isolators 0 and 1, respectively.

V. Conclusion

A switching isolator has been developed in order to overcome the problem of common ground on the front of high-resolution digitizers. The isolator incorporates a switching facility so that the isolators can be interchanged, eliminating phase error to a first-order approximation. The isolator was tested for various properties giving an isolator temperature coefficient of less than 14 ppm/°C for room temperatures; CMRR of 99.2, 79.1, and 59.2 dB at 1, 10, and 100 kHz, respectively; a 1-kHz nonlinearity corrected to within 4 μV; and a gain stability of 85 ppm at frequency of 100 kHz.

It is worth noting the significant difference between the two isolators tested. Isolator 1 has a 3 ppm/°C lower temperature coefficient, a 1.9-dB improvement on CMRR, and a 1% higher gain at 100 kHz. Collectively, these variations between the two isolators show that there is some benefit in testing multiple AD215 and selecting those with the best characteristics.

The highest contributor to the uncertainty present at 100 kHz is crosstalk through one input. A remedy to reduce crosstalk would be to only apply lower frequency components on this input. Limiting the relevant input of the isolator to 10 kHz and using the other input for frequencies up to 100 kHz would reduce the potential crosstalk from −84 to −93 dB.

References

[1] H. E. van den Brom, Z. Marais, D. Hoogenboom, R. van Leeuwen, and G. Rietveld, "A testbed for static electricity meter testing with conducted EMI," in *Proc. Int. Symp. Electromagn. Compat. (EMC Eur.)*, Sep. 2019, pp. 603–608.

[2] J. R. Pickering and P. S. Wright, "A new wattmeter for traceable power measurements at audio frequencies," *IEEE Trans. Instrum. Meas.*, vol. 44, no. 2, pp. 429–432, Apr. 1995.

[3] J. Konjevod, R. Malaric, M. Jurcevic, P. Mostarac, and M. Dadic, "Comparison of digitizers for high-precision sampling power meters," *IEEE Trans. Instrum. Meas.*, vol. 69, no. 6, pp. 3719–3728, Jun. 2020, doi: 10.1109/TIM.2019.2941260.

[4] G. Rietveld *et al.*, "Characterization of a wideband digitizer for power measurements up to 1 MHz," *IEEE Trans. Instrum. Meas.*, vol. 60, no. 7, pp. 2195–2201, Jul. 2011.

[5] T. Hagen and I. Budovsky, "Development of a precision resistive voltage divider for frequencies up to 100 kHz," in *Proc. CPEM*, Daejeon, South Korea, Jun. 2010, pp. 195–196.
[6] B. Voljc and M. M. Lindic, "Measurement of AC current with coaxial current shunts," in *Proc. Conf. Precis. Electromagn. Meas.*, Broomfield, CO, USA, Jun. 2008, pp. 540–541.
[7] Texas Instruments. *IS0124 Datasheet*. Accessed: Nov. 11, 2020. [Online]. Available: https://www.ti.com/lit/ds/symlink/iso124.pdf
[8] S. S. Mirfakhraei, Y. Audet, A. Hassan, M. Ali, M. Nabavi, and M. Sawan, "A CMOS MAGFET-based programmable isolation amplifier," in *Proc. 18th IEEE Int. New Circuits Syst. Conf. (NEWCAS)*, Montreal, QC, Canada, Jun. 2020, pp. 9–13, doi: 10.1109/NEWCAS49341.2020.9159790.
[9] Aanalog Devices. *AD215 Data Sheet*. Accessed: Aug. 12, 2019. [Online]. Available: https://www.analog.com/media/en/technical-documentation/data-sheets/AD215.pdf
[10] P. N. Davis and P. S. Wright, "An isolator to eliminate grounding issues for wideband power measurements," in *Proc. Conf. Precis. Electromagn. Meas. (CPEM)*, Denver, CO, USA, Aug. 2020, pp. 1–2.
[11] TE Connectivity. *P2 Relay V23079 Data Sheet*. Accessed: Nov. 11, 2019. [Online]. Available: https://docs.rs-online.com/0efa/0900766b81398066.pdf
[12] J. Milman, *Microelectronics: Digital and Analog Circuits and Systems*. Tokyo, Japan: McGraw-Hill Kogakusha, 1979.

Peter N. Davis received the M.Phys. degree from the University of York, York, U.K., in 2009, and the Fd.Eng. degree in electrical power engineering from Aston University, Birmingham, U.K., in 2013.

He spent a brief period with local government before joining National Grid, in 2011, on an engineering training scheme. In 2013, he joined the National Physical Laboratory, Teddington, U.K., where he is currently a Senior Research Scientist.

Paul S. Wright received the B.Sc. and Ph.D. degrees in electrical and electronic engineering from the University of Surrey, Surrey, U.K., in 1987 and 2002, respectively.

He spent three years as a Research Fellow with the University of Surrey, where he was involved in the field of spacecraft sensors and attitude control. This was followed by three years with the Central Electricity Research Laboratory, where he was involved in advanced control systems. In 1992, he joined the National Physical Laboratory, Teddington, U.K., where he is currently a Principle Research Scientist, specializing in ac measurements and waveform analysis. He is a Coordinator of the EU Project Measurement Tools for Grid Stability and Quality Management of which this work is part.